RESEARCH ARTICLE

Proposal of a Skin Temperature Measurement System Based on Digital Thermometers

GABRIEL GASPAR[1,2], **JURAJ DUDAK**[1,2], **MAGDALENA MIKOLAJCIKOVA**[3], **AND DANIEL GURIN**[3]

[1]Research Centre, University of Zilina, 010 26 Zilina, Slovakia
[2]Faculty of Materials Science and Technology, Slovak University of Technology in Bratislava, 917 24 Trnava, Slovakia
[3]Faculty of Health Care, Slovak Medical University in Bratislava, 974 01 Banská Bystrica, Slovakia

Corresponding author: Gabriel Gaspar (gabriel.gaspar@uniza.sk)

ABSTRACT The representation of temperature measurement methods is worldwide, as is the number of industries that use them. Their utilization allows one to assess the object's temperature relatively accurately and further according to the defined dependencies to evaluate its condition. In the medical sector, non-invasive temperature measurement methods are increasingly gaining ground. In our work, we focus on the design of a system for measuring skin temperature using digital DS18B20 thermometers. The technical design consists of the mechanical design of the sensor housing based on the requirements of healthcare professionals, the design of a 1-wire bus active pull-up driver with improved features, and the user software, allowing for the future implementation in various, not necessarily medical environments. The main contribution lies in optimizing the hardware design concerning the components' parameters and surge protection. In the medical field, the aim was to compare changes in skin temperature in the shoulder region depending on the type of muscle contraction during static and dynamic components of movement and to record the thermal work of the muscle during activity in real-time. We experimented by applying temperature sensors to the deltoid muscle of the dominant limb in a temperature environment of 25.76 °C. In the experimental measurements, we demonstrated that during the three selected muscle work movements, there was a temperature change in the respective regions of the deltoid muscle for each of the three, which the temperature sensors could capture. Our results were statistically significant when comparing the baseline values, and the highest temperature reached. The level of significance $\alpha \leqslant 0.05$ and a low percentage of errors were valid.

INDEX TERMS 1-wire, measurement, microcontroller, non-invasive measurement, system, temperature, temperature sensors, thermoregulation, thermodiagnostics.

I. INTRODUCTION

Temperature and its changes in the human body result from physiological and pathological changes. Regulation of body temperature is one of the basic mechanisms of homeostasis.

The associate editor coordinating the review of this manuscript and approving it for publication was Adamu Murtala Zungeru.

Advances in the measurement of body temperature are part of research in thermoregulation [1]. The results of several scientific studies have confirmed that health disorders such as chronic stress, insomnia, Alzheimer's disease, Parkinson's disease and many others affect one's body temperature [2], [3]. Skin temperature measurement can be used in the management of diseases of the internal organs [4], the

musculoskeletal system [5], or the skin itself [6]. During exercise, heat is generated in the muscles, which leads to an increase in muscle temperature. This increase becomes apparent within just a few seconds of repeated muscle contraction, proving that muscle temperature is an indicator of muscle metabolism. Muscle temperature is the most crucial factor in determining the outcome of the exercise, mainly during short-duration, high-intensity exercise. Knowledge of muscle temperature during work and exercise is critical to achieving performance improvement. Also, cooling affects the relationship between speed and force production, which means that at a specific force, the muscles' speed of movement or contraction decreases after cooling. This also means that maximal force and power in cooled muscle occurs with a slower muscle contraction rate than in thermoneutral muscle [7]. During short-term exercise, power output increases from 2% to 5% with a 1°C increase in muscle temperature. However, performance will decrease if there is an increase in core temperature, i.e., hyperthermia. An increase in muscle temperature can increase muscle strength. However, this is not a linear relationship, as there is a ceiling above which increasing the ambient temperature does not improve maximal performance. High-velocity movements are more temperature dependent than low-velocity movements. This assumption is supported by the fact that dynamic exercises are more affected by temperature than isometric contractions [8]. Measuring muscle temperature is time-consuming, invasive, and expensive [7]. Non-invasive temperature measurement is also increasingly gaining popularity as it is inexpensive, has a wide range of applications, and the measurements' evaluations are immediately usable. Some can also work with values such as heart rate and others. Yarden [9] argues that non-invasive methods of measurement at surface sites are more comfortable for the patient. However, there may be a deviation between the point of measured temperature and the body core temperature. Skin temperature measurement for detecting superficial muscle activity is used more in sports than in physiotherapy, so we decided to address this issue. Contact (liquid thermometer, silicon foil) and non-contact (infrared thermometer, thermal imager) devices for surface temperature measurement are available [10], [11]. The possibility of the skin being affected by contact devices or sensors must be considered, according to McRae [12], [13]. The sensor must also be placed in a suitable location to prevent heat loss. The most commonly used system in musculoskeletal diagnostics is the thermal imaging camera. The disadvantage is tracking within a single plane. For temperature detection for musculoskeletal diagnostics, in many cases, we need information from multiple planes simultaneously. Murugeswari et al. have researched monitoring the body temperature of cattle using an innovative infrared photodiode thermometer [14]. They claim it could be used for long-term monitoring of core body temperature, which is shown to be safe as it provides better precision for inferring the core body temperature. Another view on non-invasive measurements gives Yang et al. in [15]. With

the help of advanced technologies, physiological signals have been detected, measured, and processed using multiple technical formats, such as wearable sensors. The prospects of next-generation wearable electronics for individualized health monitoring, assistive robotics, and communication are discussed in [16]. Authors claim that critical health data monitoring, such as body temperature, wrist pulse, and blood glucose, can be retrieved and evaluated using next-generation electronic devices fabricated with advanced materials and innovative strategies. Our research aimed to design a system that uses a non-invasive temperature measurement for application in physiotherapy. Subsequently, test the system in different aspects, taking into account for use in physiotherapy, where it could find a wide application in thermo-diagnostics, either as a primary or complementary method. Based on the review of available technologies and our previous experience with 1-wire based solutions [17], [18], [19], [20], we chose the contact method using DS18B20 [21] digital thermometers as a measurement technology. Such sensors have various uses in temperature measurements [22], [23], [24]. With the unambiguous identifier of the final sensors using the built-in identifier, they allow the identification of their position at a specific point on a patient's body. Using such digital thermometers is innovative in the context of deployment in medical applications. The digital thermometer provides 9-bit to 12-bit Celsius temperature measurements and has an alarm function with nonvolatile user-programmable upper and lower trigger points. The communication method over a 1-wire bus requires only one data line (and ground) for communication with a microcontroller. In addition, the DS18B20 can derive power directly from the data line, eliminating the need for an external power supply. Available solutions for 1-wire sensor data acquisition generally address short bus lengths and do not address device surge protection or current draw detection. Because of our proposed solution's possible more comprehensive application, we decided to address and solve these issues. Such a solution includes developing software for communication, measurement, and display of measured data. Our proposal also addresses this part based on the end users' requirements.

II. MATERIALS AND METHODS
This section describes the details of materials and methods for both parts of the system design: the technical and the medical aspects. The technical and medical aspects use the standard methods for experimental measurements described in the text below.

A. TECHNICAL PART OF THE PROPOSED SOLUTION
Since our team has previous experience using DS18B20 digital thermometers, we decided to use this solution for application in the medical environment. In [17], our design utilizes 1-wire technology, which allows connecting multiple temperature sensors on a single twisted pair cable under certain conditions. The basis of 1-wire technology is a serial protocol that uses a data line and a ground reference for
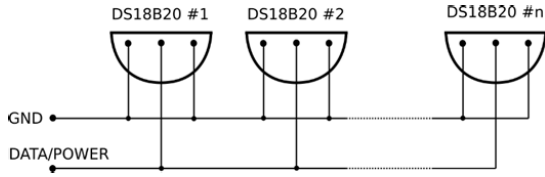
FIGURE 1. DS18B20 in a parasitic connection.

TABLE 1. The memory map of the DS1820 temperature sensor.

Byte	Scratchpad	EEPROM
Byte 0-1	Temperature registers	Not available
Byte 2	TH Register or User Byte 1	User Byte 1 (UB_H)
Byte 3	TH Register or User Byte 2	User Byte 2 (UB_L)
Byte 4	Configuration register	Configuration register
Byte 5-8	Reserved	Not Available

FIGURE 2. Experimental design of sensors in parasitic connection.

FIGURE 3. DS18B20 housing design.

communication. Additional wire for device power is optional. The 1-wire master initiates and controls communication with one or more 1-wire slave devices on the 1-wire bus. Each 1-wire slave device has a unique, unchangeable, factory-programmed 64-bit identification number that serves as the device address on the 1-wire bus. The 8-bit family code, as a subset of the 64-bit ID, identifies the type and functionality of the device. Most 1-wire devices allow one to obtain power for their operation from the 1-wire bus, which is called a parasitic power mode. In this case, the device does not need a third wire, and a single wire is shared for communication and power to the device. The 1-wire bus can be found in many IoT devices, which was another reason for our choice of sensor type DS18B20. Furthermore, implementing a 1-wire protocol on a selected microcontroller is trivial in the case of a custom solution. The sensors are available in packages with the dimensions of standard transistors (TO-92) and IC (TSOC, TDFN, SOT23). We decided to use the variant in the TO-92 package as it is more economically advantageous and allows more accessible work in laboratory conditions. The sensor connection will use parasitic wiring, as depicted in Fig. 1. With standard pull-up resistor wiring, the 1-wire bus, depending on the parameters of the cabling used, allows a length of up to approximately 100 meters with eight connected sensors. This limitation represents a significant factor for longer 1-wire buses.

In addition to the commonly used 64-bit sensor ID, we decided to use two free bytes of the nonvolatile memory of the DS18B20 sensor. These are used to set the upper and lower limits for the alarms that are used in temperature-critical applications shown in Table 11. In our design, they carry additional user-defined information about the individual sensor. The stored value is in the format: value $= UB_H * UB_L$. The stored user-defined value has a width of 16 bits and can be further utilized by the user.
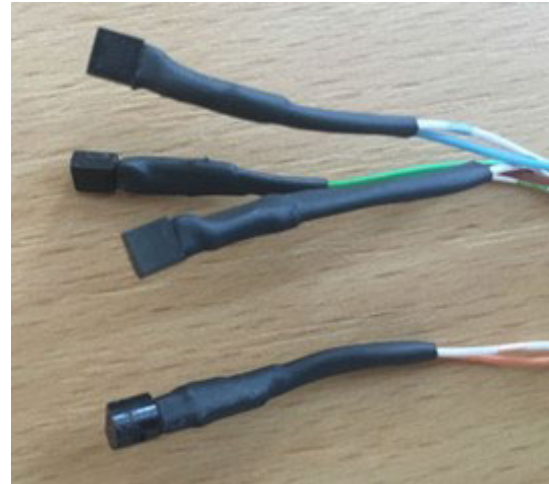
B. PROPOSED SOLUTION FOR TEMPERATURE MEASUREMENTS ON PATIENTS

For measuring the skin temperature of the patients, we decided to use the parasitic connection of the sensors. Each sensor was soldered to a connecting cable with a length of 3 meters. To verify functionality, we used an implementation with a parasitic DS18B20 connection, while bare connections were isolated using heat shrink wrap in Figure 2. However, such an embodiment did not meet the requirements for medical sensors and was thus used strictly for functionality verification.

In a subsequent step, we designed housing to store the DS18B20, including the necessary space to insert the lead cable and the solder joints in Figure 3.

Fixing the sensor and wiring positions in the designed housing and filling the remaining space in the housing was accomplished using liquid silicone rubber. As seen in the cross-section of the housing in Figure 4, the DS18B20 is positioned flush with the housing surface.

The fixation of the sensor to the patient's body was maintained as a fixation with adhesive tape, based on the
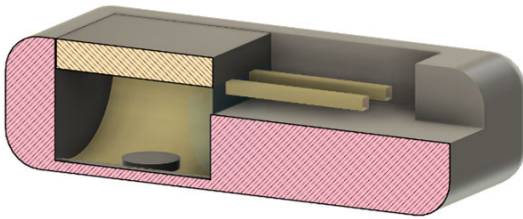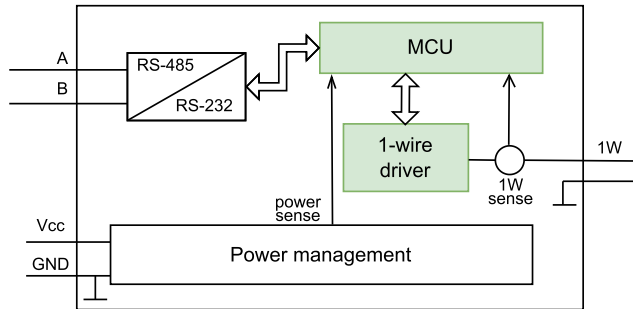
FIGURE 4. DS18B20 housing cross-section.

FIGURE 5. OWB module block diagram.

FIGURE 6. Utilized STM32F070F6 peripherals.

requirements of the cooperating health professionals. This method is simple and inexpensive, and precise positioning of the sensor is possible according to the needs of the measurement.

C. PROPOSAL OF A ONE-WIRE BOOSTER MODULE

The design of a one-wire booster (OWB) module could be described as a 1-wire bus driver with an improved properties design. Considering the limitations in the common use of the 1-wire bus, especially concerning the length of the bus and the number of connectable sensors, it was decided to design our device to eliminate these shortcomings. The block diagram of the proposed module is shown in Figure 5. The OWB design was not intended for use in the medical field only. On the contrary, the device's design is to be utilized universally in various application areas.

The 1-wire technology supports two ways to connect the sensors to the bus. Standard wiring uses three wires, where one wire is for communication, and the remaining two wires are for powering the device. The parasitic mode uses two wires, where one wire is dedicated to mutual communication and device power, and the other is reserved for GND connection. From an economic point of view, it is possible to save on cabling for large installations. This method seems suitable for use in the medical field and many other application areas.

1) OWB COMMUNICATION INTERFACE AND A MICROCONTROLLER

We chose RS485 as the communication interface. For the conversion of RS485 to RS232, with which the selected microcontroller works, the SN65HVD10 circuit was used. It is a half-duplex converter between RS-485 and RS-232.
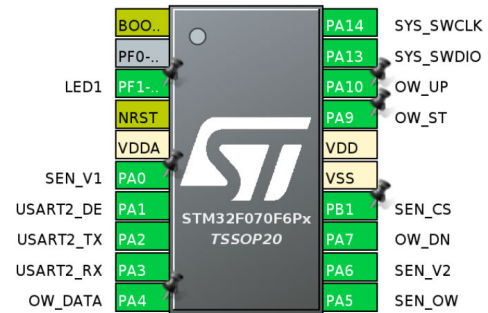
The basic parameters of this circuit, which determine the limits of the communication interface of the OWB module, are:

- Number of inputs/outputs: 1/1
- Communication mode: half duplex
- Supply voltage: 3.3VDC
- Max. transmission speed: 32 Mbps
- Overvoltage protection: -9VDC to 14VDC
- Max. operating current Icc: 15.5 mA

For the design of the OWB module was chosen the STM32F070F6 microcontroller in the TSSOP20 design, i.e., in a 20-pin package. The basic features of this chip are as follows:

- ARM® 32-bit Cortex®-M0 CPU, frequency up to 48 MHz
- Memories: 32kB FLASH, 6kB RAM
- 15 I/O pins with 5V tolerant capability
- One 12-bit, 1.0 μs ADC (up to 16 channels)
- 5 timers
- one I2C interface
- two USART interfaces
- one SPI interface

The peripheral usage of the STM32F070F6 microcontroller is shown in Figure 6:

- Status indication: LED1 indicates when the device is active, performs the measurement on the sensors, or communicates with the host device.
- Analog/Digital Converter (ADC) - 4 channels are used to monitor the supply voltage level (SEN_V1), the voltage on the 1-wire bus (SEN_V2), the current draw measurement on the 1-wire bus (SEN _CS), and a fourth channel is used for 1-wire bus length detection (SEN_OW).
- UART, the communication interface of the OWB module. It is used in an asynchronous mode (USART2_ TX/RX).
- I/O pins - OW_DATA, OW_UP/ST/DN - are used for the 1-wire bus driver.
- Debug interface (SYS_SWCLK/SWDIO) - used only during the actual development.

2) A MODIFIED 1-WIRE BUS DRIVER

The 1-wire bus operates at 5VDC. This voltage represents the inactive state of the bus. In a parasitic connection, the DQ line
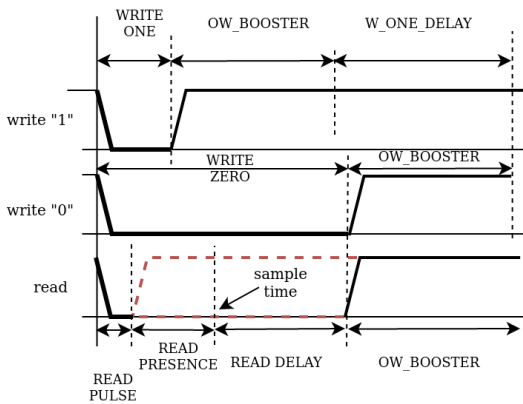
FIGURE 7. 1-wire communication timing parameters, master implementation.

TABLE 2. 1-wire bus timing parameters for standard and long bus lengths.

Parameter	Timing for a standard bus [μs]	Timing for a long bus [μs]
TIME_SLOT	70	85
WRITE_ZERO	45	60
WRITE_ONE	10	12
WRITE_ONE_DELAY	45	60
WRITE_DELAY	10	5
READ_PULSE	6	12
READ_PRESENCE	9	8
READ_DELAY	30	40
OW_BOOSTER	25	25

(communication pin) is used to power the sensors and communicate since the VCC and GND pins are connected to zero potential. When communicating, the sensors operate thanks to a parasitic power supply, meaning they can communicate only for a specific, finite time. After the communication is over, the state is restored when the bus voltage level is at a value corresponding to log.1. At this time, a built-in circuit is activated that recharges the supercapacitor, which serves as a power source for the sensor. With a 1-wire bus length of more than several meters, a voltage drop is observable on the bus. For lengths of more than tens of meters, the capacity of the communication bus is negatively affected. In order to avoid signal attenuation, with no communication on the bus or when the bus level needs to be quickly changed from low level to 5V, a 'hard' 5V is connected to the bus in order to quickly change the bus state to an inactive state - i.e., to log. 1 state.

3) ADAPTIVE 1-WIRE BUS TIMING

A modified timing scheme has been proposed to implement the 1-wire protocol in a master mode in Figure 7. All of these time intervals can be configured in software. Modifying them allows communication on the long 1-wire bus to be adapted accordingly. When using a long bus, it is crucial to extend the READ_PULSE time to a value such that all connected 1-wire slave devices can detect the start of the communication. Another critical parameter is WRITE_ZERO, by which the master node sends the value "0". The sample parameters for the standard and long 1-wire bus are shown in Table 2. The parameters for the long bus were empirically found for a 600m long bus.

Table 11. In our design, they carry additional user-defined information about the individual sensor. The stored value is in the format: value = $UB_H * UB_L$. The stored user-defined value has a width of 16 bits and can be further utilized by the user.

For a long bus, the OW_BOOSTER time at which the dynamic pull-up driver is activated is crucial. By activating

this pull-up driver, we achieve a fast change in voltage level. In the current design of the OWB module, a constant value of OW_BOOSTER = 25μs has been chosen. From this value, the other times are derived according to the following equations (1, 2):

$$\text{WRITE\_ZERO} = \text{TIME\_SLOT} - \text{OW\_BOOSTER} \quad (1)$$

$$\text{WRITE\_ONE\_DELAY} = \text{TIME\_SLOT} - (\text{WRITE\_ONE} + \text{OW\_BOOSTER}) \quad (2)$$

The following equations (3, 4) apply to the timing of the read operation:

$$\text{READ\_PRESENCE} + \text{READ\_PULSE} = 18 \quad (3)$$

$$\text{READ\_DELAY} = \text{TIME\_SLOT} - (\text{READ\_PULSE} + \text{READ\_PRESENCE} + \text{OW\_BOOSTER}) \quad (4)$$

WRITE_ONE and WRITE_ZERO parameters are equal to 10μs and 45μs, respectively, when using a short bus (up to 50m). When using a more extended bus, there is a signal attenuation and a reflection from the end of the bus during communication - this is visible in Figure 8. This reflection causes the level change from 5V to 0V or vice versa to be delayed by up to 10μs to 20μs. This phenomenon cannot be prevented, but it is possible to adjust the 1-wire bus timing (by increasing the WRITE_ZERO value) to allow enough time to reliably reduce the bus voltage level when the bit is read.

4) 1-WIRE BUS SHORT-CIRCUIT DETECTION AND CURRENT LOAD MONITORING

Short-circuit detection on the 1-wire bus is a functionality of the OWB module to indicate incorrect sensor wiring or the accidental connection of the data and ground wires. A short circuit is indicated by a warning LED. When a short circuit is detected, the OWB module communicates, but the error code DEVICE_HW_ERROR_2 (0×08) is returned
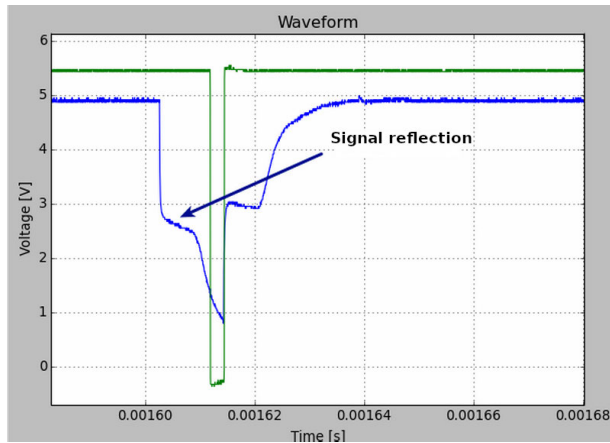
FIGURE 8. Signal reflection on a long 1-wire bus.

FIGURE 9. Current load monitoring circuitry.

for functions associated with the 1-wire bus. Short-circuit detection is accomplished by directly connecting a voltage divider with a 1:3 resistor ratio to the 1-wire bus. This circuit should be designed to affect communication on the 1-wire bus minimally. With this in mind, the resulting divider resistance is 133kΩ. If the high level of the 1-wire bus is 5V, the current flowing through the voltage divider is 37μA. Monitoring the current load of the 1-wire bus is essential when using sensors with higher power requirements in parasitic mode. These are in the order of units of mA per module. The ZXCT1022 circuit [25] was used to monitor the 1-wire bus load current. The ZXCT1022 is a Low Offset High-side Current Monitor used to eliminate the need to disrupt the ground plane when sensing a load current. It provides a fixed gain of 100 for applications with minimal sensing voltage. The very low offset voltage enables a typical accuracy of 3% for sense voltages of only 10mV, giving better tolerances for little sense resistors necessary at higher currents. Figure 9 shows the wiring diagram of the current load monitoring circuitry.

The value of the R$_{sense}$ resistor was chosen to be 50mΩ. The equation (5) between the output voltage and the actual current is the following:

$$V_{out} = I \cdot R_{sense} \cdot k \quad (5)$$

where R$_{sense}$ = 0.05Ω and k = 100 (gain of the circuit ZXCT1022). For the current flowing, applies the equation (6):

$$I = \frac{V_{out}}{k \cdot R_{sense}} \quad (6)$$

After the enumeration:

$$I = \frac{V_{out}}{100 \cdot 0.05\Omega} = \frac{V_{out}}{5\Omega}$$

The ADC converter in the microcontroller reads the V_{out} value. In Figure 6, the pin marked SEN_CS is used for this functionality.
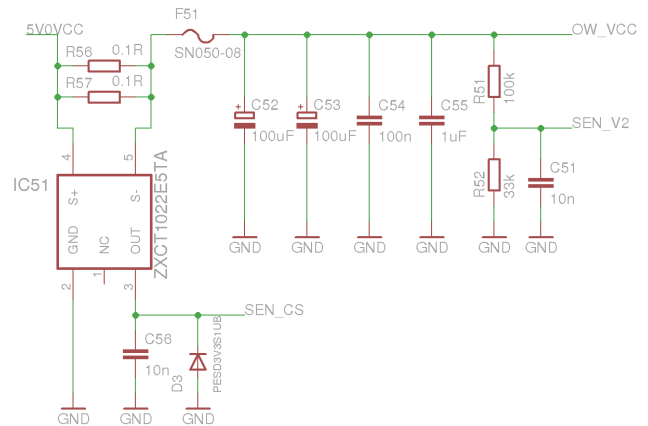
5) ENHANCED 1-WIRE BUS ACTIVE PULL-UP
The solution for implementing a 1-wire bus active pull-up driver [26] is supplied by Maxim Integrated – the manufacturer of DS18B20 sensors. Figure 10 provides the electrical schematics.

The OWB hardware module contains an enhanced version of this proposal. The wiring diagram of this proposal is shown in Figure 11. The main differences between the OWB module design and a standard controller with an active pull-up driver are as follows:

- Selection of components with more suitable parameters for the given purpose:
    – The transistors used are designed for switching, controlled from logic circuits. In the original design, BSS84 and 2N7002 transistors are used. In the OWB design, IRLML2244 transistors with low switching losses are used.
    – The transistor switching resistance (S-D) in the switched state is significantly lower - 54mΩ for our modified design vs. 10Ω for the original design.
- Special integrated circuits (U61) with charge pumps are used to control the switching transistors for a faster transistor state change. This part is absent in the original design.
    – U61 - The MCP14E11 [27] is a high-speed MOSFET driver, capable of providing 3.0A of peak current. The dual inverting, dual noninverting, and complementary outputs are directly controlled from TTL or CMOS (3V to 18V). These devices also feature low shoot-through current, near-matched rise/fall times, and propagation delays, which make them ideal for high switching frequency applications.
- Protection of the circuitry against unwanted bus overvoltage is implemented by a particular diode (D53) combined with a fast diode (D52).
    – D53 - This diode is explicitly designed to protect sensitive electronic equipment from voltage transients induced by lightning and other transient
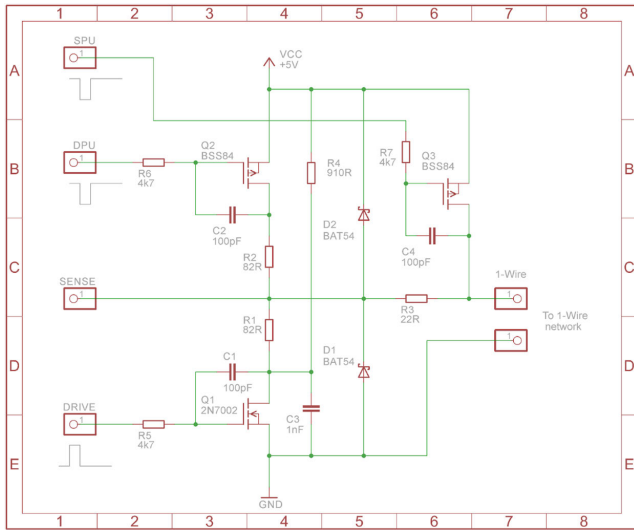
FIGURE 10. 1-wire bus active pull-up driver.

FIGURE 11. The enhanced 1-wire bus driver.

voltage events. Fast response time: typically, less than 1.0ps from 0 Volts to VBR.

- D52 - The MBR0530 [28] uses the Schottky barrier principle with a large area metal-to-silicon power diode. They are ideally suited for low voltage, high-frequency rectification or as freewheeling and polarity protection diodes in surface mount applications where compact size and weight are critical to the system.

- A fast comparator U71 shapes the measured signal (OW_O).
  - The U71 - MCP14E11 circuit is used in the comparator function.

- For the sampled signal from the bus (OW_O), a window comparator (IC81A) is in a circuit with a fast operational amplifier to shape this signal.
  - IC81A - This comparator has extremely high input impedance (typically greater than $10^{12}\Omega$), allowing direct interfacing with high-impedance sources. The outputs are n-channel open-drain configurations and can be connected to achieve positive-logic wired-AND relationships.

- The supply voltage for the 1-wire bus is isolated by a polymeric return fuse (F51 in Figure 9) to protect the control circuits.

- The circuit is supplemented by low ESR capacitors (C5x in Figure 9) to cover short-term pulse withdrawals.

- Sensing the current drawn by the 1-wire bus - SEN_CS in Figure 9 - to evaluate the error condition when the bus current flows outside the allowed limit.

- Voltage detection on the 1-wire bus to detect short circuits or low voltage on the 1-wire bus. SEN_V2 signal in Figure 9. This condition can occur when an accidental short circuit or a damaged sensor is connected.
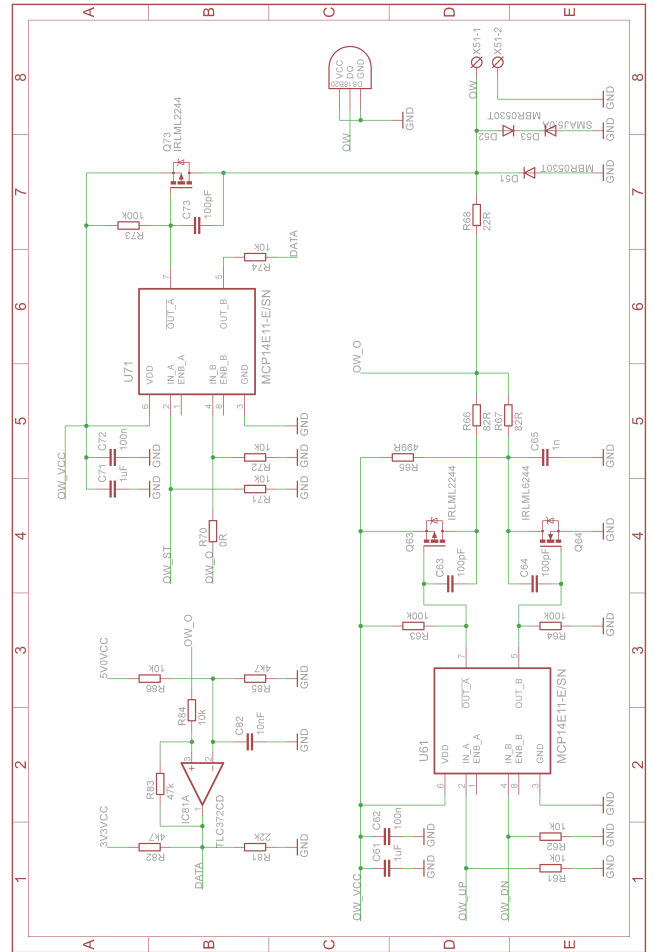
D. MERULA SOFTWARE APPLICATION

The Merula application in Figure 12 is a desktop application for direct measurement on the measurement modules of the proposed measurement system. It supports connectivity via USB (virtual COM port) or IP communication. The primary purpose of this application is to run on-demand measurements while communication with multiple measurement modules is possible.

Once connected, information about the connected measurement module is displayed. On the left of the application window is a tree view of the hierarchy structure: a list of measurement modules with connected sensors or additional interfaces. The measurement module "DCB_1820" is shown in Figure 12, which contains the interface "OW_boost" representing the 1-wire bus. On this bus, four sensors were detected. After clicking on the measurement module, the "Board info" section displays the selected measurement module: module ID, SW/HW version, module designation, module name, date of manufacture, and module address. Similarly, if a sensor is selected in the sensor system tree, its properties are displayed in the "Sensor info" section: sensor name and sensor address. Selecting "Active" causes the
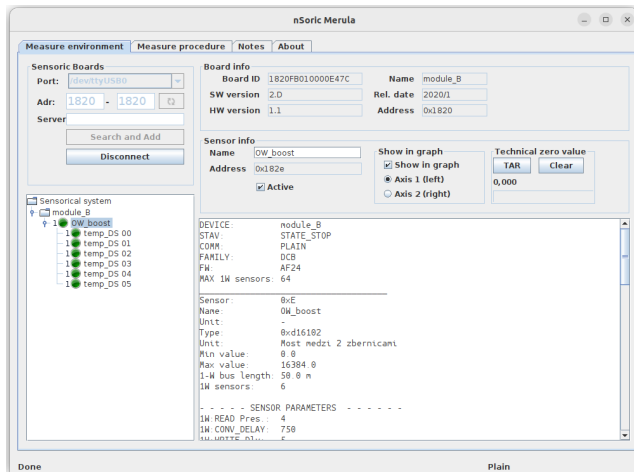
FIGURE 12. Merula application interface.

TABLE 3. Sensors positioning on the participant's body.

Sensor	Measurement point
SENSOR I. (brown)	Pars acromialis proximal part
SENSOR II. (green)	Tuberositas deltoidea (muscle tendon)
SENSOR III. (orange)	Pars clavicularis
SENSOR IV. (blue)	Belly of the deltoid muscle, approximately in the middle

sensor to be included in the measurement. When displaying the measured data in a live graph, it is possible to choose whether the measured value will be displayed and, if so, which axis will be used. At the bottom of the window is an area with informative communication statements. Those come up during the measurement module initialization and the actual measurement on the module.

E. MEDICAL PART OF THE PROPOSED SOLUTION

For medical applications, we measured skin temperature over the working muscle. Monitoring changes in skin temperature over time indicates the blood supply directly to the area and indirectly the work of a particular muscle. Therefore, multiple modes of muscle contraction were chosen. The above-designed system can simultaneously connect multiple sensors from any side of the patient's body (limit of the thermal camera) and with minimal influence of the skin temperature by the sensor itself (limit of the silicon foil). The main benefit of using more sensors is the possibility of placing them on specific parts of the skin and reading the temperature simultaneously from all places. It is possible to localize changes and their course over time, which is not possible with a thermal camera or any other device used so far. The changes measured by us monitored the temperature values over individual parts of the deltoid muscle during its different activation. Based on this, it is possible to monitor changes and differences in the involvement of individual parts of the monitored muscle.

The measurement procedure consists of 2 phases:

- **Settling**. After attaching the sensors to the part of the skin to be examined, it is necessary to wait for the sensor's temperature and the human body's temperature to equalize. During this time, temperature readings are taken from the sensors. When the temperature has stabilized, this phase is finished. The last temperature readings on the sensors are taken as a reference.

- **Measurement**. The measured temperature values are evaluated as the change concerning the steady-state temperatures from the first step.

The reason for using this method of measurement is that the DS18B20 thermometers have an absolute measurement error of $\pm 0.5°C$. However, the resolution of the sensor is $0.0625°C$. This way of measurement gives a relative temperature change with a resolution of $0.0625°C$. For high-performance thermal cameras standardly used in medicine, the measurement uncertainty is $\pm 1°C$, $\pm 2°C$. Thus, the proposed system meets medical requirements in terms of measurement accuracy.

1) TEST GROUP

The test group consisted of 10 participants of the 3rd year of full-time physiotherapy study at the Faculty of Health Sciences of SZU, based in Banská Bystrica. 6 males and 4 females participated in the measurement. The lower age limit of the participants was 21 years, and the upper age limit was 23 years. The mean age of the participants was 21.9 ± 0.51 years, the mean body weight 69.1 ± 11.74 kg and the mean body height 173.6 ± 6.86 cm. BMI in the cohort averaged 22.78 ± 2.73. None of the subjects had a history of severe upper limb injury or any other injury that could affect the measurement results. The participants were in good physical condition, nine testers were recreational athletes, and one had been active in athletics for 4 years.

2) WORK METHOD

We chose the dominant upper limb, specifically the musculus deltoideus muscle region, to test the device. We chose this place of application because of the ease of access. The deltoid muscle is anatomically one of the superficially located muscles. We also considered that this area is sparsely hairy and does not form a barrier when the sensors are attached to the skin. Using Kinesio tape, every single sensor was attached to the skin at the sensing point. The representation of the sensors on the different regions of the deltoid muscle is elaborated in Table 3.

We tested the system in three different components. We chose to compare the thermal work of the muscles:

- Isometric contraction, in the starting position of 90-degree abduction at the shoulder joint with the elbow joint extended and the palm facing down.
- Isometric contraction with a weight, in a baseline position of 90-degrees abduction at the shoulder joint with

FIGURE 13. Isometrics with weight.

FIGURE 14. Example of a graph created in Merula (cyclic movements with weight).

FIGURE 15. OWB module prototype.

the elbow joint extended and the palm facing down, where participants held a gender-appropriate weight in the test hand in Figure 13.

- A cyclic movement with the same weight as the second component. Here, the movement was based on the upper limb extended at the elbow joint to a position of 90-degree abduction at the shoulder joint and extended at the elbow joint with the weight held steady with the palm facing downwards.

In the first two movements, during isometrics, we chose a minute endurance of the tested limb in the starting position. The cyclic movement described above was performed 10-times in three repetitions with 30-second pauses between repetitions. All measurements were performed seated in a chair. We always started the measurement after fixing each sensor at the predetermined place, especially after the program read all four sensors. After each movement was made, we always let the measurement run for some more time so that the sensors could pick up the increase in temperature changes. We separately respected each test's performance, as the time in which the temperature changes occurred differed slightly for each one. The severity differed between the sexes. We measured the movements in the following order:

1) isometrics without load,
2) isometrics with load,
3) cyclic movement with load.

We left small pauses between each movement. After each measurement, we also saved a graphic representation of the measurement progress from the Merula application in Figure 14. We did this for every single component of testing that we measured and also for each participant.

III. RESULTS

From the technical aspect of our work, we can state that experimental measurements have shown that with a conventional pull-up resistor connection, the usable length of the 1-wire bus is approximately 100 meters. The hardware design of our 1-wire driver overcomes these limitations. Experimental measurements show that a bus length of more than 500 meters [19] can be achieved with reliable communication with up to 128 connected DS18B20 sensors. The
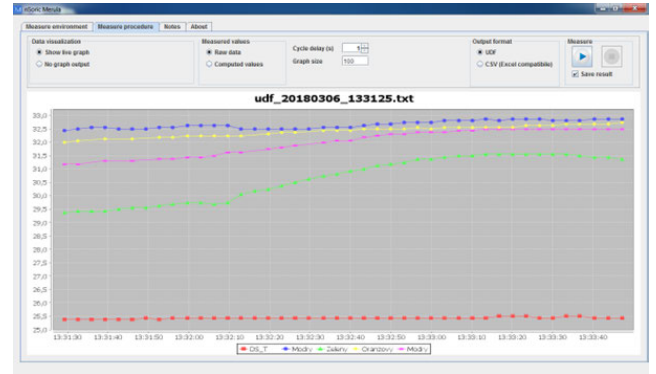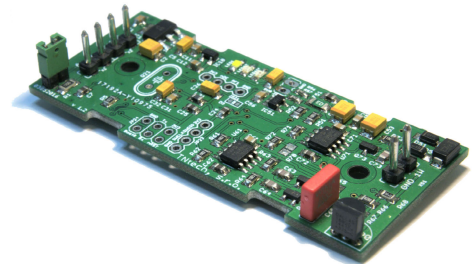
TABLE 4. Statistical evaluation of values in isometrics without load.

Parameter [°C]	SENSOR I.	SENSOR II.	SENSOR III.	SENSOR IV.
Average temperature vt	31.36	31.14	31.68	31.43
Standard deviation	1.26	1.21	0.59	0.96
Average temperature nt	32.08	31.93	32.19	32.20
Standard deviation	0.78	0.79	0.55	0.60
Average difference vt and nt	0.72	0.74	0.51	0.78
Standard deviation	0.59	0.59	0.17	0.48
t-test vt and nt = p [-]	0.0027	0.0014	< 0.001	0.0005

OWB module prototype in Figure 15 allows both standard and parasitic wiring modes to be used but primarily aims at parasitic sensor wiring. This method saves wiring costs and, by comparison of the performed experimental measurements, is as efficient as the standard wiring method.

We constantly evaluated *vt* (initial temperature) and *nt* (highest temperature reached) as the average of 10 measurements. SENSOR III recorded the highest *vt* (31.68), with the lowest variance (0.59) from the mean value in Table 4, visualized in Figure 16.

In the subsequent measurement, our results were based on a higher mean vt than in the previous. This was again most evident in SENSOR III (32.08), with the lowest standard deviation (0.64). In the parametric Student's paired
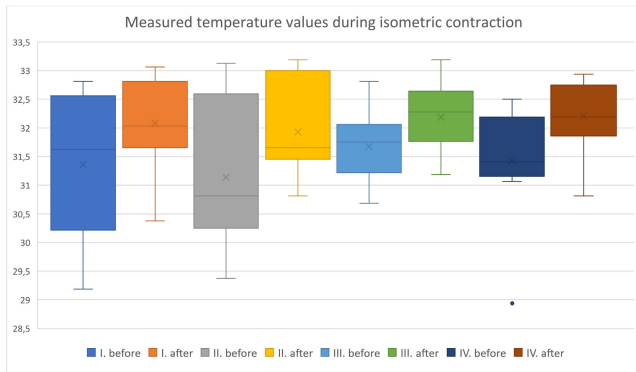
FIGURE 16. Temperature values during isometric contraction.

TABLE 5. Statistical evaluation of values in isometrics with a load.

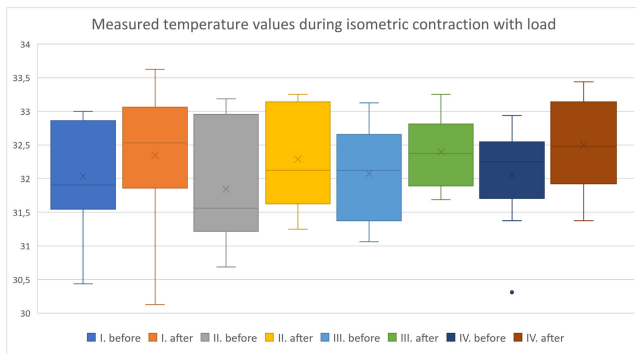| Parameter [°C]	SENSOR I.	SENSOR II.	SENSOR III.	SENSOR IV.
Average temperature vt	32.04	31.84	32.08	32.06
Standard deviation	0.78	0.83	0.64	0.72
Average temperature nt	32.34	32.23	32.39	32.50
Standard deviation	0.93	0.70	0.49	0.65
Average difference vt and nt	0.31	0.44	0.32	0.44
Standard deviation	0.35	0.30	0.18	0.44
t-test vt and nt=p [-]	0.0133	0.0008	0.002	0.0009

FIGURE 17. Temperature values during isometric contraction with a load.

t-test, we obtained the highest of all (0.0133) for SENSOR I. However, $p<0.05$ was still valid; for this measurement, we obtained statistically significant values with a low % of errors in Table 5, visualized in Figure 17.

For this measurement, we worked with an average ambient temperature of 25.78°C. The time from the resting value to the highest measured value was 1.4 minutes. The average initial temperatures were higher than in the previous measurement (Figure 17). The highest value achieved during testing is achieved on the SENSOR IV (32.38°C). The lowest temperature increase occurred at SENSOR I (0.22). The detailed

TABLE 6. Statistical evaluation of values during cyclic movements with a load.

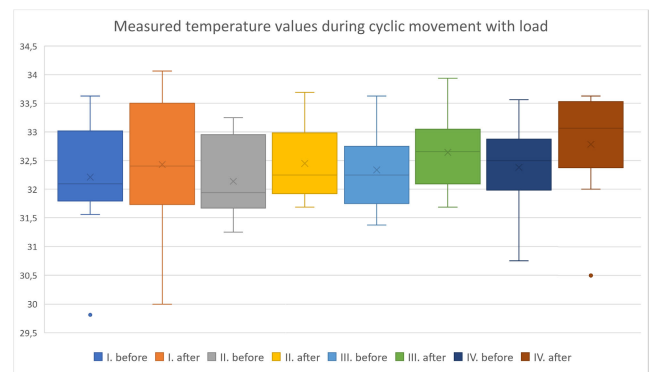| Parameter [°C]	SENSOR I.	SENSOR II.	SENSOR III.	SENSOR IV.
Average temperature vt	32.21	32.14	32.34	32.38
Standard deviation	0.03	0.64	0.64	0.78
Average temperature nt	32.43	32.50	32.64	32.80
Standard deviation	1.14	0.63	0.62	0.92
Average difference vt and nt	0.22	0.31	0.31	0.40
Standard deviation	0.25	0.29	0.26	0.41
t-test vt and nt=p [-]	0.0150	0.0053	0.0032	0.0083

FIGURE 18. The temperature rises during cyclic movements with a load using average values.

measurements are summarized in Table 6 and visualized in Figure 18.

For these measurements, we worked with the average value (25.90°C) recorded by the OWB and considered the average temperature of the environment where the measurement was performed. The highest value was recorded at SENSOR I (0.0150), and the other values were also significant.

IV. DISCUSSION

From a technical point of view, this work has eliminated several shortcomings in designing the 1-wire bus active pull-up driver. Utilization of appropriate components optimized the switching transistors and provided short-circuit and over-voltage protection for the device. Due to the current trend of securing recently unaddressed lower layers of techno-logical units, securing the communication of the proposed solution with the higher-level system is planned for the future enhancements. It has already been partially addressed in [29], where there was implemented the security of the uBUS protocol. When designing thermometer housings for use in medical environments, the emphasis must be placed on work with multiple designs to ensure comfort for the patient and the most negligible impact of the fabricated sensors on heat transfer. In the future, we would like to validate multiple

biocompatible materials and designs with multiple dimensions in housing function. The software part of the solution called Merula is built universally and currently suits experimental measurements well. In the future, we would like to implement the storage of measured data in a cloud solution with the possibility of visualizing the measured data. This functionality is also used in other fields, not only in medical applications. The novelty of our solution lies mainly in the following:

- A design of a special 1-wire bus driver (booster), which makes it possible to utilize a bus length of up to 500m,
- 1-wire bus length detection and automatic adjustment of bus timing parameters,
- short-circuit detection on the 1-wire bus,
- automatic switching of bus timing according to the bus length,
- upstream communication via RS-485,
- supply voltage ranges from 5.5V to 12V (version A) or from 7.5V to 24V (version B).

From a medical perspective, it was found that during each type of muscle work activity, there was a change in temperature in given areas over the deltoid muscle, which was measured by temperature sensors.

Compared to standard methods of measuring skin temperatures, such as thermal imaging cameras or IR thermometers, the presented system has the following features:

- guaranteed measurement on the same measuring points,
- guaranteed measurement on all sensors at the same time,
- configurable measurement frequency - max 1 Hz,
- independence of the positioning of the sensors on the human body. Compared to the solution with a thermal imaging camera, where the monitored part of the body must be visible to the camera,
- elimination of disturbing ambient parameters such as ambient temperature, relative humidity, light intensity, light flashes, and the like.

Considering the features above, this system is a fitting complement to existing options for medical skin temperature measurements.

During isometric contraction without weights, the muscle likely did not contract long enough for the muscle to become sufficiently engorged for the sensors to detect a more pronounced temperature increase on the skin. The graphs generated by our proposed Merula application at each measured movement clearly showed time and temperature values that corresponded to them. According to Lloyd et al. [30] Changes in skin temperature are reflected on the skin after a specific time, to which was adapted the length of the temperature sensing. We performed the measurements consecutively, starting with isometrics without weights and ending with cyclic motion. It turned out that already in isometry with weights, it was measured with a higher initial temperature, and thus the difference of the increase was minor, contrary to expectations. The lowest baseline temperature when measuring isometrics without weights on the SENSOR I. was

29.19°C in one participant. For isometry with weights in the same participant, it was 30.44°C, so the difference was 1.25°C. It was found that more time was needed between measurements to allow the sensors to cool down and avoid biased values. It would potentially show a more significant temperature increase and, thus, a value difference. Studies [8] confirm that muscle fiber fatigue decreases when their temperature increases from low temperature to more physiological values. According to a study by Flouris et al. [7], a large heat generation occurs during exercise, leading to increased muscle temperature with just a few seconds of repeated contraction. With measurements, it was found that even after a few seconds, the sensors recorded a temperature increase. However, to compare the temperature measured at the skin surface and the muscle under the skin, it would be helpful to introduce a temperature probe (intramuscular) at the site to measure the regional temperature as described by Flouris et al. [7] in his study. Measured values on the body surface showed delayed responses with a comparison of internal changes at rest during and after exercise. Based on the measured values, muscle temperature could be predicted as a dependent variable for other participants. The surface temperature was measured using an iDisc, which was applied to the skin using a neoprene disc to prevent temperature minimization between the skin and the environment. This disk was taped to the patient's body using surgical tape. Indeed, it was confirmed that there is local insulation of the skin. The temperature under the disc is increased due to thermogenesis. Based on these findings, in our testing, leakage could have occurred due to the low insulation of the sensor attachment on the skin, which could be most evident during cyclic movements. By applying a sensor housing, this can be mitigated. If initiated from the observation that dynamic movements are more influenced by temperature than isometric contractions [8], this was not the case for our measured group. A possible explanation is that during the cyclic movement, which was measured last, there was still a residual temperature; therefore, the baseline temperature was the highest of all the measurements, and the difference before and after the load was the smallest. Another reason stated by Binzoni et al. [31] may be that the change in the local muscle does not induce the same effect under different physiological conditions, for example, the type of muscle contraction. Another reason may be the small number of subjects. The weight, which were chosen to be different concerning sex, could theoretically have influenced the rate of increase in the highest temperature measured. As the performance level of individuals was not tested, an appropriate weight for each individual was not separately determined. However, this may not have affected isometric activity, as Mallette et al. [32] described. The highest mean values of temperature increases, shown in the tables, were recorded at two sensors: the SENSOR III (pars clavicularis) and the SENSOR IV (the belly of the deltoid muscle). The long-known fact can be considered that during an abduction, the deltoid muscle exerts less force

to move the limb, than the force it exerts in the form of pressure on the humerus in the joint, fixing the humeral head in the socket [33]. Based on the previous observation, such temperature changes may represent the stereotype of movement in participants and, thus, the degree of activity of the individual fibers in the execution of the movement.

V. CONCLUSION

From a technical point of view, our task was to design a measurement system using digital thermometers with appropriate software support for a medical application. We decided to extend the task and design the system universally for use in several areas without limitation to the target, in this case, the medical area. For the application in the medical area, we designed a sensor housing intending to minimize the temperature conditions of the patient's body. Next, a hardware solution for an advanced 1-wire bus driver has been proposed with several improvements in the component base and safety and diagnostic features. Finally, the Merula software was designed to be equally versatile for measurements and recording data to CSV files. We see future extensions possible, especially in software, in storing measured data in a database and their further processing and sharing. From a medical point of view, our main objective in the pilot study was to test the proposed system for selected measurements with the possibility of further use in thermodiagnostics in physiotherapy practice. According to the algorithm of the measurement procedure defined in section E, the measurements result in temperature changes concerning the steady-state values measured at the beginning of the experiment. Based on the results, we believe that the proposed system is suitable for the defined purposes of thermodiagnostics, taking into account that temperature measurements in a non-invasive way are among the measurements that are neither difficult nor expensive and with a wide range of applications. Temperature sensors can record changing temperatures over time with great sensitivity. The time interval of the total measurement for one participant was about 15 minutes and increasing temperature values over time are consistent with physiological findings. This type of diagnosis could serve as a primary or complementary method. The results open up possibilities for further testing in practical applications such as sports, training, alternative medicine, or neurological diagnoses. However, we cannot forget possible improvements and recommendations in testing and considering new findings and studies from thermodiagnostics worldwide.

INFORMED CONSENT STATEMENT

Informed consent was obtained from all subjects involved in the study.

REFERENCES

[1] R. Niedermann, E. Wyss, S. Annaheim, A. Psikuta, S. Davey, and R. M. Rossi, "Prediction of human core body temperature using non-invasive measurement methods," *Int. J. Biometeorol.*, vol. 58, no. 1, pp. 7–15, Jan. 2014, doi: 10.1007/s00484-013-0687-2.

[2] L. Durrer, "Case study: Non-invasive core body temperature measurements during sleep and daily life with greenteg gskin bodytemp kit measured on the wrist," Electro Opt. Compon., Santa Rosa, CA, USA, Tech. Rep., 2020.

[3] J. L. Sanchez-Jimenez, I. Aparicio, J. L. Romero-Avila, C. Bellot-Arcís, R. M. Cibrián Ortiz de Anda, and J. I. Priego-Quesada, "Skin temperature measurement in individuals with spinal cord injury during and after exercise: Systematic review," *J. Thermal Biol.*, vol. 105, Apr. 2022, Art. no. 103146, doi: 10.1016/j.jtherbio.2021.103146.

[4] M. Bottaro, N.-U.-H. Abid, I. El-Azizi, J. Hallett, A. Koranteng, C. Formentin, S. Montagnese, and A. R. Mani, "Skin temperature variability is an independent predictor of survival in patients with cirrhosis," *Physiol. Rep.*, vol. 8, no. 12, 2020, Art. no. e14452, doi: 10.14814/phy2.14452.

[5] J. B. Ferreira-Júnior, S. F. N. Chaves, M. H. A. Pinheiro, V. H. S. Rezende, E. D. S. Freitas, J. C. B. Marins, M. G. Bara-Filho, A. Vieira, M. Bottaro, and C. M. A. Costa, "Is skin temperature associated with muscle recovery status following a single bout of leg press?" *Physiol. Meas.*, vol. 42, no. 3, Mar. 2021, Art. no. 034002, doi: 10.1088/1361-6579/abe9fe.

[6] X. Jiang, X. Hou, N. Dong, H. Deng, Y. Wang, X. Ling, H. Guo, L. Zhang, and F. Cai, "Skin temperature and vascular attributes as early warning signs of pressure injury," *J. Tissue Viability*, vol. 29, no. 4, pp. 258–263, Nov. 2020, doi: 10.1016/j.jtv.2020.08.001.

[7] A. D. Flouris, P. Webb, and G. P. Kenny, "Noninvasive assessment of muscle temperature during rest, exercise, and postexercise recovery in different environments," *J. Appl. Physiol.*, vol. 118, no. 10, pp. 1310–1320, May 2015, doi: 10.1152/japplphysiol.00932.2014.

[8] S. Racinais and J. Oksa, "Temperature and neuromuscular function," *Scandin. J. Med. Sci. Sports*, vol. 20, no. 3, pp. 1–18, Oct. 2010, doi: 10.1111/j.1600-0838.2010.01204.x.

[9] M. Yarden, "Non-invasive temperature measurement," U.S. Patent 7 597 668 B2, Oct. 6, 2009.

[10] S. G. Holt, J. H. Yo, C. Karschimkus, F. Volpato, S. Christov, E. R. Smith, T. D. Hewitson, L. J. Worth, and P. Champion De Crespigny, "Monitoring skin temperature at the wrist in hospitalised patients may assist in the detection of infection," *Internal Med. J.*, vol. 50, no. 6, pp. 685–690, Jun. 2020, doi: 10.1111/imj.14748.

[11] S. Yanfen, M. Liangxiao, Z. Jiang, Q. Conghui, W. Yanxia, T. Ling, L. Chunhua, Y. Hongwen, L. Yuqi, and S. Jiashan, "Comparative study on skin temperature response to menstruation at acupuncture points in healthy volunteers and primary dysmenorrhea patients," *J. Traditional Chin. Med.*, vol. 37, no. 2, pp. 220–228, 2017, doi: 10.1016/S0254-6272(17)30048-1.

[12] B. A. MacRae, S. Annaheim, C. M. Spengler, and R. M. Rossi, "Skin temperature measurement using contact thermometry: A systematic review of setup variables and their effects on measured values," *Frontiers Physiol.*, vol. 9, o. 29, Jan. 2018, doi: 10.3389/fphys.2018.00029.

[13] B. A. MacRae, C. M. Spengler, A. Psikuta, R. M. Rossi, and S. Annaheim, "A thermal skin model for comparing contact skin temperature sensors and assessing measurement errors," *Sensors*, vol. 21, no. 14, p. 4906, Jul. 2021, doi: 10.3390/s21144906.

[14] S. Murugeswari, K. Murugan, S. Rajathi, and M. Santhana Kumar, "Monitoring body temperature of cattle using an innovative infrared photo-diode thermometer," *Comput. Electron. Agricult.*, vol. 198, Jul. 2022, Art. no. 107120, doi: 10.1016/j.compag.2022.107120.

[15] B. Yang, X. Li, Y. Hou, A. Meier, X. Cheng, J.-H. Choi, F. Wang, H. Wang, A. Wagner, D. Yan, A. Li, T. Olofsson, and H. Li, "Non-invasive (non-contact) measurements of human thermal physiology signals and thermal comfort/discomfort poses—A review," *Energy Buildings*, vol. 224, Oct. 2020, Art. no. 110261, doi: 10.1016/j.enbuild.2020.110261.

[16] A. S. Farooq and P. Zhang, "A comprehensive review on the prospects of next-generation wearable electronics for individualized health monitoring, assistive robotics, and communication," *Sens. Actuators A, Phys.*, vol. 344, Sep. 2022, Art. no. 113715, doi: 10.1016/j.sna.2022.113715.

[17] G. Gaspar, J. Dudak, M. Behulova, M. Stremy, R. Budjac, S. Sedivy, and B. Tomas, "IoT-ready temperature probe for smart monitoring of forest roads," *Appl. Sci.*, vol. 12, no. 2, p. 743, Jan. 2022, doi: 10.3390/app12020743.

[18] G. Gaspar, S. Sedivy, J. Dudak, and M. Skovajsa, "Meteorological support in research of forest roads conditions monitoring," in *Proc. 2nd Int. Conf. Smart Electron. Commun. (ICOSEC)*, Oct. 2021, pp. 1265–1269, doi: 10.1109/ICOSEC51865.2021.9591632.

[19] J. Dudak, P. Tanuska, G. Gaspar, and P. Fabo, "ARM-based universal 1-wire module solution," *J. Sensors*, vol. 2018, Mar. 2018, Art. no. 5268247, doi: 10.1016/j.sna.2022.113715.

[20] J. Dudak, G. Gaspar, and G. Michalconok, "Extension of 1-wire measuring system SenSys," in *Proc. 15th Int. Conf. (MECHATRONIKA)*, Dec. 2012, pp. 1–4.

[21] *Ds18b20 Programmable Resolution 1-Wire Digital Thermometer*, document 19-7487; Rev 6; 7/19, Maxim Integrated, San Jose, CA, USA, 2022.

[22] H. Lu, Y. Li, S. Mu, D. Wang, H. Kim, and S. Serikawa, "Motor anomaly detection for unmanned aerial vehicles using reinforcement learning," *IEEE Internet Things J.*, vol. 5, no. 4, pp. 2315–2322, Aug. 2018, doi: 10.1109/JIOT.2017.2737479.

[23] D. Guangyue, L. Meili, Y. Feng'e, W. Xiaohong, D. Xiaomeng, and S. Benlan, "Study on synchronous method of multi-sensor data acquisition in space based on single-bus digital temperature sensor," in *Proc. Int. Conf. Adv. Mech. Syst. (ICAMechS)*, Dec. 2022, pp. 189–193, doi: 10.1109/ICAMechS57222.2022.10003379.

[24] S. Kumra, "A survey of acceptability and use of IoT for patient monitoring," in *Proc. Int. Conf. Mach. Learn., Big Data, Cloud Parallel Comput. (COM-IT-CON)*, May 2022, pp. 30–36, doi: 10.1109/COM-IT-CON54601.2022.9850512.

[25] *ZXCT1022 (Current Monitors Master Table)*, Diodes Incorporated, Plano, TX, USA, 2022.

[26] *Guidelines for Reliable Long Line 1-Wire Networks*, Maxim Integrated, San Jose, CA, USA, document AN148, 2014.

[27] *MCP14E9/10/11*, Microchip Technology, Chandler, CA, USA, document DS25005A, 2011.

[28] *MBR0530 Schottky Rectifier*, ON Semiconductor, Phoenix, AZ, USA, document MBR0530/D, 2019.

[29] J. Dudak, G. Gaspar, S. Sedivy, P. Fabo, L. Pepucha, and P. Tanuska, "Serial communication protocol with enhanced properties–securing communication layer for smart sensors applications," *IEEE Sensors J.*, vol. 19, no. 1, pp. 378–390, Jan. 2019, doi: 10.1109/JSEN.2018.2874898.

[30] A. Lloyd, L. Picton, M. Raccuglia, S. Hodder, and G. Havenith, "Localized and systemic variations in central motor drive at different local skin and muscle temperatures," *Amer. J. Physiol.-Regulatory, Integrative Comparative Physiol.*, vol. 313, no. 3, pp. R219–R228, 2017, doi: 10.1152/ajpregu.00055.2017.

[31] T. Binzoni and D. Delpy, "Local temperature changes and human skeletal muscle metabolism," *J. Physiol. Anthropol. Appl. Hum. Sci.*, vol. 20, no. 3, pp. 159–174, 2001, doi: 10.2114/jpa.20.159.

[32] M. M. Mallette, L. A. Green, G. J. Hodges, R. E. Fernley, D. A. Gabriel, M. W. R. Holmes, and S. S. Cheung, "The effects of local muscle temperature on force variability," *Eur. J. Appl. Physiol.*, vol. 119, no. 5, pp. 1225–1233, May 2019, doi: 10.1007/s00421-019-04112-x.

[33] V. Lanik, *Kineziológia*. Martin, Czechoslovakia: Osveta, 1990.

JURAJ DUDAK received the Ph.D. degree from the Faculty of Informatics and Information Technologies, Slovak University of Technology in Bratislava, in 2011.

He is dedicated to low-level programming for sensors. He is an expert in the design and implementation of software solutions. His specialization is code creation for single-chip microprocessors, design and creation of desktop multiplatform applications, and design of database solutions. He has published scientific and technical papers in national and international conference proceedings and journals.

Dr. Dudak is a member of the International Association of Engineers (IAENG) and the editorial board of *International Journal of Sensors and Sensor Networks* (IJSSN).

MAGDALENA MIKOLAJCIKOVA received the master's degree in study program physiotherapy from the Alexander Dubcek University of Trencin in 2021.

She is currently a Physiotherapist with the healthcare sector in Slovakia, where she is participating in the education of students. She works as an External Teacher with The Faculty of Healthcare in Banska Bystrica. She was the author of the "Pilot Study Equipment Proposal for Thermodiagnostics in Physiotherapy" (bachelor thesis), in 2018.

GABRIEL GASPAR received the Ph.D. degree in the field of automation from the Faculty of Materials Science and Technology, Slovak University of Technology in Bratislava, Trnava, Slovakia, in 2016.

Since 2020, he has been the Managing Director of the Transport Infrastructure Research Division, Research Centre, University of Zilina, Zilina, Slovakia. He has published scientific and technical papers in national and international conference proceedings and journals. He is the sole author or a coauthor of several IPRs. His research and development interests include the field of low-level microprocessor programming, PCB design, software applications in the field of sensory systems, and the preparation of physical experiments to verify proposed sensors.

Dr. Gaspar is a member of the International Association of Engineers (IAENG) and the editorial board of *International Journal of Sensors and Sensor Networks* (IJSSN).
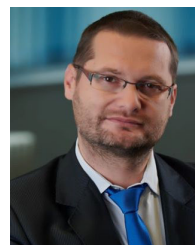
DANIEL GURIN received the Ph.D. degree in kinanthropology from the Faculty of Sport Studies, Masaryk University in Brno, Czech Republic, in 2016.

He has been the Vice-Dean of the Science, Research, and Foreign Relations, Faculty of Health Care with a seat in Banska Bystrica, Slovak Medical University in Bratislava, Slovakia, since 2017, where he has been the Head of the Department of Physiotherapy, since 2013. He works and publishes scientific articles in the field of sport and rehabilitation.

Dr. Gurin is a member of the Scientific Council of the Faculty of Health Care and the Working Group for Other Health Professions for the Ministry of Education, Science, Research and Sports of the Slovak Republic.

● ● ●